Published in final edited form as:
Clin Cancer Res. 2014 January 1; 20(1): 199–212. doi:10.1158/1078-0432.CCR-13-0762.

Direct inhibition of Retinoblastoma phosphorylation by Nimbolide causes cell cycle arrest and suppresses glioblastoma growth

Swagata Karkare[#1,3], **Rishi Raj Chhipa**[#1], **Jane Anderson**[1], **Xiaona Liu**[1], **Heather Henry**[1], **Anjelika Gasilina**[2], **Nicholas Nassar**[2], **Jayeeta Ghosh**[2], **Jason P Clark**[2], **Ashish Kumar**[2], **Giovanni M. Pauletti**[3], **Pradip K Ghosh**[4], and **Biplab Dasgupta**[1,*]

[1]Departments of Oncology, Cincinnati Children's Hospital Medical Center, OH

[2]Experimental Hematology and Cancer Biology, Cincinnati Children's Hospital Medical Center, OH

[3]James L. Winkle College of Pharmacy, University of Cincinnati, OH

[4]Maryville University, St. Louis, MO.

[#] These authors contributed equally to this work.

Abstract

Purpose—Classical pharmacology allows the use and development of conventional phytomedicine faster and more economically than conventional drugs. This approach should be tested for their efficacy in terms of complementarity and disease control. The purpose of this study was to determine the molecular mechanisms by which nimbolide, a triterpenoid found in the well-known medicinal plant *Azadirachta indica* controls glioblastoma (GBM) growth.

Experimental Design—Using *in vitro* signaling, anchorage-independent growth, kinase assays, and xenograft models, we investigated the mechanisms of its growth inhibition in glioblastoma.

Results—We show that nimbolide or an ethanol soluble fraction of *A. indica* leaves (Azt) that contains nimbolide as the principal cytotoxic agent is highly cytotoxic against GBM *in vitro* and *in vivo*. Azt caused cell cycle arrest, most prominently at the G1-S stage in GBM cells expressing EGFRvIII, an oncogene present in about 20-25% of GBMs. Azt/nimbolide directly inhibited CDK4/CDK6 kinase activity leading to hypophosphorylation of the retinoblastoma (RB) protein, cell cycle arrest at G1-S and cell death. Independent of RB hypophosphorylation, Azt also significantly reduced proliferative and survival advantage of GBM cells *in vitro* and in tumor xenografts by downregulating Bcl2 and blocking growth factor induced phosphorylation of Akt, Erk1/2 and STAT3. These effects were specific since Azt did not affect mTOR or other cell cycle regulators. *In vivo*, Azt completely prevented initiation and inhibited progression of GBM growth.

Conclusions—Our preclinical findings demonstrate Nimbolide as a potent anti-glioma agent that blocks cell cycle and inhibits glioma growth *in vitro* and in *vivo*.

[*]Corresponding Author, **Contact**: Biplab Dasgupta PhD, Assistant Professor of Pediatrics, Division of Oncology, Cincinnati Children's Hospital Medical Center, 3333 Burnet Avenue, Cincinnati OH 45229, Biplab.dasgupta@cchmc.org, Phone: 513-8031370, Fax: 513-8031083.

Conflict of Interest: We disclose that there is no conflict of interest with regard to the submitted manuscript.

INTRODUCTION

Glioblastoma multiforme (GBM) is one of the most common primary brain tumors in the adult population. Despite substantial progress in patient outcome in other human cancers and significant advancement in our understanding of the genetics and pathology of GBM, decades of therapy have failed to drastically change survival. The most frequent (>40%) gain of function event in primary GBM is amplification of the epidermal growth factor receptor (EGFR), often associated with a ligand-independent constitutively active mutant receptor called *EGFRvIII* (1). Two tumor suppressors frequently lost in GBM are *INK4a/ARF* that regulates the retinoblastoma (*RB*) protein and *PTEN* that regulates *PI3K* (2, 3). Because multiple growth factor pathways are often upregulated in GBMs including the PI3K-Akt, MEK-Erk1/2 and the JAK-STAT3 pathways (4), it is being argued that for certain types of cancers (including GBM), development of drugs that target multiple pathways could be more effective than pathway-specific drugs.

Phytochemicals derived from medicinal plants are time-tested for their curative properties against a plethora of chronic human diseases. Because of their safety, long term use, and their ability to target multiple pathways, there is a renewed interest to understand their molecular mechanisms of action. Phenolic compounds and isothiocyanates induce cell cycle arrest by stabilizing p21 and p53 (5, 6), while curcumin and resveratrol (both in cancer clinical trials) induce apoptosis by downregulating Bcl2 and upregulating Bax (6, 7). Organosulphur derivatives from garlic also exert anticancer effects by downregulating NF-κB (8). Recently, Trabectedin, a natural product of marine origin (also in clinical trial) induced apoptosis specifically in tumor macrophages (9). *Azadirachta Indica*, is one such medicinal plant with tremendous commercial interest and with long history of use for over 2000 years in primary health care in India and neighboring countries (10, 11). Fractionated extracts of its leaves (known as IRAB) with registered U.S. Pat. No. 5370873 is registered and marketed in Africa as IRACARP for its broad-spectrum anti-cytoadhesion activity and its beneficial effects in HIV/AIDS (12, 13). By comparing the cytotoxic potency of the bioactive compounds isolated from the leaf extract it was found that nimbolide is the principal cytotoxic component of the leaf extract (14). Nimbolide is a tetranortriterpenoid consisting of a classical limonoid skeleton with a α,β- unsaturated ketone system and a δ-lactonic ring (13, 14). The ethanol-soluble fraction of *Azadirachta Indica* leaves (henceforth called Azt) as well as nimbolide has been shown to exert several biological activities including anti-satiety response (15), anti-malarial (16), anti-HIV (13) and anti-cancer response (17).

Azt/nimbolide exhibits anti-cancer properties against a variety of tumor cells including neuroblastoma, osteosarcoma, leukemia and melanoma cells (18-21). These cancer cells are variously affected, likely due to the interaction of Azt with the unique pathways mutated in these cells. Some of the pathways involved in Azt action include cell cycle arrest at G0/G1 (21), increased ROS production (19), activation of caspases, modulation of the levels of cell cycle inhibitors (22) and suppression of NF-κB activity (20). In animal tumor models, nimbolide (10–100 mg/kg) has been shown to exhibit chemopreventive activity against 7,12-dimethylbenz[α]anthracene (DMBA)-induced oral carcinogenesis (17, 23). The αβ -unsaturated ketone structure of nimbolide is linked to its anti-cancer property, while amide derivatives modified on the lactone ring enhanced its cytotoxicity (14). Because the cytotoxic properties of Azt/nimbolide has not been thoroughly tested in GBM, we examined its effectiveness against human glioma cells, especially cells with overexpression of the oncogene EGFRvIII, found in up to 25% of primary GBM patients (1).

In this study, we report that by inhibiting RB phosphorylation and blocking multiple growth factor pathways relevant to GBM, Azt/nimbolide is an extremely potent cytotoxic agent that kills GBM cells *in vitro* and suppresses tumor initiation and progression *in vivo*.

MATERIALS AND METHODS

Cell Culture

T98G, A172 and U87 cells were obtained from ATCC and G2 cells were obtained from Peter Houghton, Nationwide Children's Hospital, Columbus, OH. U87EGFR and U87EGFRvIII cells (obtained from Paul Mischel, UCLA) were maintained in puromycin (1μg/ml) and hygromycin (150 μg/ml), respectively. P9 is a primary adult GBM neurosphere line obtained from John Ohlfest, University of Minnesota. All glioma cells except P9 were cultured in DMEM with 10% FCS. P9 cells were cultured in ultra-low attachment dishes in DMEM/F12 supplemented with B27, N2, EGF and FGF. Cell viability was determined by Trypan Blue exclusion method.

Photomicrography

Images of soft agar colonies and whole brain coronal sections were taken with a Nikon AZ-100 multi-zoom microscope attached with DS-RI1 12 MP color camera and histology images were taken with a Leica DM2500 brightfield upright microscope attached with a DFC 500 12 MP color camera.

Preparation of Azt

Dried powder of *Azadirachta indica* leaves was prepared (by PKG) by drying fresh leaves at 37°C for 24h and grinding them into a powder using a mortar and pestle. Azt extract was prepared as before (23) with minor modifications. To prevent batch to batch variation, a single batch of Azt extract was prepared by soaking 40g of dry powder in 200 ml 95% ethanol (200 mg/ml) and Azt was extracted at 4°C on a shaker for five days. The extract was centrifuged and clear supernatant was filtered through a 0.2 micron filter and stored in aliquots at −20°C. Appropriate volume of this stock (200 mg/ml) was added to the culture medium to achieve 1, 2 and 4 μg/μl final concentration (for example 5ul, 10 ul or 20 ul of stock was added to 1 ml culture medium to achieve 1, 2 or 4 ug/ul final concentration).

Flow cytometry

Cell cycle distribution was performed by flow cytometry. Cells were treated with EtOH (control) or Azt (2 μg/μl for 12 hour and 1 μg/μl for 24 hour), harvested, fixed with 70 % ice cold EtOH at −20 °C for 1 h and resuspended in 0.5ml of PI/ RNAse staining buffer. Cell death analysis was done by Annexin V staining. Following labeling, cells were filtered through a 70μm Sefar Nylon Lab Pak Mesh. DNA content was analyzed on a Beckman Coulter Quanta™ SC MPL Flow Cytometer.

Anchorage independent growth

For Anchorage independent growth, 2×10^4 GBM cells were mixed with 0.7% top agar and layered on top of 1% bottom agar made in 2X DMEM with 20% FCS and antibiotics. Cells were fed with medium containing EtOH, DMSO (control) or Azt, nimbolide (Purchased from Bio Vision) every third day and allowed to grow for two weeks. Colonies were stained with crystal violet and imaged. Colony quantitation was done using Image J software.

Western blot analysis

Glioma cells were lysed with RIPA lysis buffer (20mM Tris, 10 mM EGTA, 40mM β-glycerophosphate, 1% NP40, 2.5mM $MgCl_2$, 2mM orthovanadate 1 mM PMSF, 1 mM DTT

and protease inhibitor cocktail). The following antibodies (all from Cell Signaling Technology) were used: Cleaved PARP, Bcl2, pRB, pAkt, Akt, pGSK3β**,** GSK3αβ**,** pCyclinD1, Cyclin D1, pErk1/2, Erk1/2, pSTAT3, STAT3, pS6, S6, p4EBP1, 4EBP1, Cyclin B1, P27, P21 and actin.

Nonradioactive *in vitro* kinase assay

Nonradioactive *in vitro* kinase assay was performed by examining phosphorylation on a GST-RB fusion peptide (residues 736-840). GST-RB1 construct containing residues 736-840 of RB (Addgene) was purified according to standard protocol. GST-RB1 was expressed in Rosetta 2 (DE3) pLys cells. Cells were lysed by sonication in Buffer A (20mM Tris pH8.0, 300mM NaCl). Lysate was loaded on glutathione Superflow beads (Qiagen), equilibrated with Buffer A. Following extensive wash in Buffer A, GST-RB1 was eluted with Buffer A supplemented with 50mM Glutathione. Fractions containing GST-RB1, as judged by SDS-PAGE, were pooled, dialyzed against 20mM Tris pH 8.0, 200mM NaCl, 0.1% β-mercaptoethanol and concentrated to 2mg/ml (Amicon, 10kDa cutoff). Kinase assay was conducted as previously described (24). Briefly, U87EGFRvIII were lysed with RIPA buffer, and CDK4/6 was immunoprecipitated with Cyclin D1 antibody, washed twice with RIPA buffer, once with 10 mM Tris-Hcl (pH 7.5) and 0.5 M LiCl, once with Kinase assay buffer and suspended in kinase buffer (25mM Tris-HCl pH 7.5, 5 mM β-glycerophosphate, 2 mM DTT, 0.1 mM Na_3VO_4,, 10mM $MgCl_2$). Reactions were carried out at 30°C for 45 minutes by adding GST-RB fusion protein and 250 μM ATP to the reaction mix. Reaction was terminated by adding Laemmli buffer and boiling for 5 min. Samples were resolved in 14% SDS-PAGE, and Western blot analysis was performed with phospho-$RB^{Ser807/811}$ antibody (Cell Signaling Technology).

Plasmids

Rb RBS811E mutant was made from wild type mouse Rb cDNA purchased from Open Biosystems and using Quickchange II-XL site-directed mutagenesis kit (Agilent Technologies).

In vivo Experiments

All animal procedures were carried out in accordance with the Institutional Animal Care and Use Committee-approved protocol of Cincinnati Childrens Hospital and Medical Center. Animals were monitored daily by animal care personnel. For flank *in vivo* xenografts experiments, 1.5×10^6 U87EGFRvIII cells were injected into the flanks of *nu/nu* mice. For glioma initiation experiment, cell were pretreated with EtOH (control) or Azt for 1h and injected into the flanks. Mice did not receive any further injections of EtOH or Azt. For glioma progression experiment, similar numbers of untreated cells were injected and tumors were allowed to grow for seven days. Following this, 62.5 ul of 95% ethanol or Azt (0.34 μg/g body weight) was injected directly into the tumor bed of the left and right flank respectively, every other day for eight days. To examine the effect of systemic effect of nimbolide, we injected 1.5×10^6 U87EGFRvIII cells into the flanks of *nu/nu* mice, allowed tumor seeding for three days and treated animals with nimbolide (@10μg/Kg body wt, IV) or vehicle (DMSO) every day for seven days. Tumor growth was monitored by measuring tumor volume every other day by using the formula $\pi/6 \times A \times B^2$ (A = larger diameter; B = smaller diameter). Tumors were dissected out and imaged using an iPAD 3. For intracranial xenograft experiments, U87EGFRvIII cells were infected with LeGo-Cer2 lentivirus expressing firefly luciferase or lentivirus expressing DsRed fluorescent reporter. 1×10^5 cells, unlabeled or labeled cells (depending on experimental group – see results) were injected into the cerebral cortex of male *nu/nu* mice (2mm caudal to bregma; 2 mm right of midline; 3 mm deep) using a stereotactic device. Tumor seeding was allowed for three days

following which mice received nimbolide (@ 200μg/Kg body wt, IP) or vehicle (DMSO). All animals were imaged twice – once, three days after tumor seeding before start of treatment to ensure they had similar starting signals and next, on day 14. Five minutes before imaging, mice were anesthetized and injected (IP) with luciferin (150 mg/Kg) and imaged using IVIS (Xenogen). All mice were euthanized following observation of lethargy and/or neurological symptoms. For DsRed-labeled tumors, 2 mm thick coronal brain sections were dissected and tumor area was measured using the *Image J* software.

Immunohistochemistry

Immunohistochemistry was done as previously described (24). Mice were anesthetized, perfused intracardially with 4% PBS, tumors were dissected out and processed for paraffin embedding and sectioning. Tissue sections were stained with H&E. Immunohistochemistry was performed on adjacent deparaffinized six-micron sections by using standard antigen retrieval methods. The following primary antibodies were used: Ki67 (Vector laboratories), cleaved Caspase 3, pAkt, pErk1/2, pSTAT3 (Cell Signaling Technology). Vectastain ABC kit (Vector laboratories) was used for microscopic visualization.

STATISTICAL ANALYSIS

Student's *t* test was used to calculate statistical significance with $p < 0.05$ representing a statistically significant difference. Kaplan-Meier analysis with log-rank Post-hoc test was used for survival studies.

RESULTS

Azt/nimbolide kills GBM cells in a dose dependent manner

We first compared the cytotoxic efficacy of an aqueous and an organic solvent extract of *Azadirachta indica* leaves. While the aqueous extract had no effect, a 95% EtOH extract killed T98G GBM cells in a dose dependent manner (Fig 1A). At 4μg/μl, Azt killed 100% of the cells in 20 hours under normal culture conditions. As a comparison, treatment of GBM cells for 20 hours with Temozolomide (TMZ), the adjuvant used together with radiation as part of standard of care in GBM therapy had no effect at 50 and 100μM (Fig 1B). TMZ had a slight effect at 72h (Fig S1A), which is not surprising since as shown by others (25), T98G and U87 cells are not significantly susceptible to even long exposure of 100μM TMZ alone, but is effective together with radiation. We also compared the inhibitory efficiency of Azt/nimbolide with other standard chemotherapeutic agents including DNA topoisomerase inhibitors including Etoposide, Camptothecin, another alkylating agent Mitomycin C, mTORC1 inhibitor Rapamycin, mTORC1/C2 inhibitor PP242 and the PI3K/mTOR dual kinase inhibitor BEZ235. We used these compounds at doses higher than the reported range of IC50 values for various cancer cell lines at 72h of growth (e.g., Etoposide 5-10μM, Camptothecin 0.5-1μM, Mitomycin C 3-30nM, Rapamycin 2.5-10nM, PP242 0.5-2μM, BEZ235 4-75nM). Because nimbolide killed nearly 100% of cells at 72h, we compared viability at 20h. Nimbolide was much more effective in reducing viability of U87EGFRvIII cells than any of these agents at 20h of growth (Fig S1B). This cytotoxic effect of Azt was universal, since it killed six other cell lines including two adult GBM cells that overexpresses EGFR or EGFRvIII, one adult primary GBM neurosphere line (P9) and one pediatric GBM line (G2). (Fig 1C). Photomicrographs of A172 and U87 EGFRvIII cells treated with Azt for 20 hours is shown in Fig 1D, E. The U87EGFRvIII cells rounded up (as happens to dying cells) quicker than other cells even at the lowest dose of Azt (1μg/μl). Accordingly, while the parental U87 cells did not lose viability at lower doses, 50-70% U87EGFRvIII cells were killed at 0.75 and 0.875 μg/μl Azt respectively (Fig 1F). This suggests that constitutively active signaling through the EGFRvIII oncogene likely induces

oncogenic stress and enhances vulnerability of GBM cells towards Azt. Next, we conducted similar experiments with nimbolide (Fig 1G), the principal cytotoxic component of Azt. Similar to Azt, nimbolide considerably reduced the viability of GBM cells in a dose dependent manner and again GBM cells expressing the EGFRvIII oncogene were more sensitive than other cells at 10μM concentration (Fig 1H). Taken together, these results show that nimbolide either in its purified form or as an EtOH-soluble fraction in Azt is a potent cytotoxic agent that abolishes growth of GBM cells *in vitro*.

GBM cells expressing the EGFRvIII oncogene are highly susceptible to G1-S arrest by Azt/nimbolide

To examine how Azt reduces viability of GBM cells we first conducted cell cycle analysis by flow cytometry. The most dramatic effect of Azt was on the U87EGFRvIII cells. At 12h, it caused a massive accumulation of cells at S and depletion at G1 and G2M (compare Fig 2A versus B). At 24h, compared to EtOH-treated cells, more than 90% of Azt-treated cells accumulated at G1, concomitant with a depletion of cells from S and G2M (compare Fig 2C versus D). Importantly, as shown in (Fig 2E-H), Azt did not affect the cell cycle of normal astrocytes at 12h or 24h (compare cells in S-G2M in B versus F and D versus H). Cell death in U87EGFRvIII cells was verified by flow cytometry analysis in which we observed that about 70% of the Azt-treated U87EGFRvIII cells stained positive for Annexin V (Fig 2I). Compared to EtOH, Azt also caused substantial increase in the Sub G0 population of T98G cells at both 12h and 24h (compare cells in Sub G0 in J versus K and L versus M in Fig 2) and to some extent in the U87EGFRvIII cells (compare cells in Sub G0 in A versus B and C versus D in Fig 2), but not in astrocytes (Fig 2F, H). We could not detect Sub G0 population in the Azt-treated parental U87 cells (Fig 2 N-Q). Compared to EtOH -treated cells, twice as many Azt-treated T98G cells showed accumulation in the S phase (compare S phase cells in J versus K and L versus M in Fig 2). Azt-treated parental U87 cells showed a slight increase in G1 and a reduction in the S phase (Fig 2 N-Q). Together, these results suggest that perhaps genetic variations (mutations) in GBM cells influence the nature of cell cycle arrest induced by Azt, and cells with the EGFRvIII mutation are considerably more vulnerable to Azt-mediated G1 arrest and the effect of Azt on cell cycle is specific to GBM cells.

Azt/nimbolide inhibits anchorage-independent growth of GBM cells

We showed that Azt reduces viability of GBM cells grown in monolayers. To examine if Azt is capable of inhibiting anchorage-independent growth (a key test for tumor aggressiveness and metastatic potential *in vivo*), we conducted soft agar colony formation assay. Following two weeks of growth in the presence of EtOH (control) or Azt, control cells rapidly formed large colonies, while Azt treatment significantly ($p < 0.001$) prevented colony formation in all GBM cells in a dose-dependent manner (Fig 3A-D). When added after seven days of growth, Azt still inhibited colony formation (not shown) suggesting its inhibitory effect on the progression of colony growth. Similar to Azt, nimbolide potently inhibited colony formation in a dose dependent manner (Fig 3E-H). Thus Azt and its principal cytotoxic component nimbolide are highly potent agents that inhibit anchorage-independent growth of glioma colonies *in vitro*.

Azt/nimbolide downregulates Bcl2, induces apoptosis and blocks serum-stimulated Akt and RB phosphorylation

Since Azt shifted cells to the sub G0 stage, a feature characteristic of cell death, we examined if Azt caused apoptosis. Indeed, western blot analysis using cleaved PARP3 antibody showed active Caspase-dependent cleavage of PARP3 in Azt-treated GBM cells (Fig 4A). Since Azt reduced cell viability, we examined if it affected expression of antiapoptotic cell survival proteins. Indeed, Azt robustly downregulated the antiapoptotic

protein Bcl2 in a time-dependent manner (Fig 4A). Together, these results indicate that Azt/nimbolide reduces glioma viability both by inducing cell cycle arrest and cell death.

To investigate the mechanism of G1-S arrest by Azt, we examined the key regulators of the G1-S phase. Growth factor withdrawal inactivates cyclin dependent kinases (CDKs) that upon growth factor stimulation phosphorylates and inhibits the Retinoblastoma (RB) tumor suppressor protein to allow G1-S transition. As expected, serum-stimulation caused robust RB phosphorylation which was considerably inhibited in the presence of Azt and this effect was maximal in the U87 EGFRvIII cells (Fig 4B). Azt also suppressed serum-stimulated Akt phosphorylation (Fig 4B). We initially hypothesized that probably upstream events like Akt inhibition leads to hypophosphorylation and activation of the Akt substrate GSK3β leading to phosphorylation of the GSK3β site on Cyclin D1. Phosphorylation of Cyclin D1 by GSK3β at threonine 286 enhances its ubiquitination and proteasomal degradation preventing its interaction with CDK4, and CDK4-dependent RB phosphorylation. However, despite inhibition of Akt phosphorylation by Azt, we did not observe any change in GSK3β and Cyclin D1 phosphorylation (Fig 4B). No change in protein levels of Cyclin D1, (a crucial G1 Cyclin), Cyclin B1 (a crucial G2 Cyclin), and P27, P21 (two key negative regulators of the G1-S phase) were observed.

We therefore questioned whether Azt/nimbolide directly inhibits the kinase activity of CDK4/6. To test this, CDK4/6 was immunoprecipitated from U87EGFRvIII cells with Cyclin D1 antibody and was used in a nonradioactive *in vitro* kinase reaction with a GST-RB (736-840) peptide in the presence of EtOH or DMSO (control) and Azt or purified nimbolide. Indeed, Azt/nimbolide robustly inhibited CDK4/6 activity in a dose dependent manner (Fig 4C). The highly orchestrated, cyclical phosphorylation of RB throughout the cell cycle makes RB overexpression studies difficult. Nevertheless, we generated lentiviruses expressing RB (S811E), potentially creating a phosphomimetic. We used control GFP virus or RBS811E to examine whether an RB phosphomimetic mutant would rescue Azt and nimbolide's growth inhibitory effects. DMSO-treated RBS811E expressing U87EGFRvIII cells grew similar to control virus infected cells and both Azt and nimbolide reduced proliferation of control virus infected cells. However, RBS811E expressing cells showed nearly 70% rescue when treated with Azt/nimbolide (Fig 4D) suggesting that CDK4/6 inhibition is likely an important mechanism of Azt/nimbolide's growth inhibitory actions. Our results demonstrate that by directly inhibiting CDK4/6 activity, Azt/nimbolide causes a sustained (chronic) inhibition of RB phosphorylation and cell cycle arrest at G1-S and glioma cells carrying the EGFRvIII oncogene are particularly susceptible to this arrest by Azt/nimbolide.

Azt/nimbolide-induced cytotoxicity is irreversible

We have shown that chronic exposure of GBM cells to Azt/nimbolide suppresses growth. To interrogate if Azt-induced growth suppression is reversible, we exposed GBM cells to Azt (2μg/μl) or 95% EtOH (1% final) or PBS (control) for 1 or 2 hours. Cells were washed in drug-free medium, and equal numbers of live cells were reseeded in drug-free growth medium for 72 hours. While EtOH - treated cells grew similar to PBS-treated cells (although there was some effect of EtOH itself), nearly 100% of the Azt-treated cells failed to survive and proliferate (Fig 5A), suggesting that acute exposure to Azt/nimbolide causes irreversible changes that are detrimental to the growth and survival of GBM cells.

To investigate the signaling pathways that might be acutely affect by Azt, we examined several growth factor pathways. GBM cells were serum-starved and stimulated with serum for 1 or 2 hours in the presence of EtOH (control) or Azt (2μg/μl). Azt strongly inhibited phosphorylation of Akt, Erk1/2, STAT3 and RB (Fig 5B) – signaling pathways vital for proliferation and survival of GBM cells. This inhibition showed some specificity since the

mTOR pathway remained uninhibited as revealed by unchanged phosphorylation of S6 and 4EBP1, two bonafide downstream effectors of mTOR (Fig 5B).

We next tested whether the acute *in vitro* irreversible growth suppressive effect of Azt is also true *in vivo*. We predicted that probably tissue microenvironment would allow Azt-treated cells to survive and form tumor masses. $1.5x10^6$ live U87EGFRvIII cells (treated as above) were injected into the flank of nude mice. While EtOH treated cells formed large tumor mass, contrary to our prediction, GBM cells acutely treated with Azt completely failed to survive and grow as xenografts (Fig 5C, D). Together, our results demonstrate that Azt exerts an irreversible cytotoxic effect on GBM cells *in vitro* that cannot be rescued *in vivo*.

Azt/nimbolide inhibits GBM tumor growth *in vivo*

So far we have shown that Azt/nimbolide markedly reduces GBM cell viability *in vitro*. To verify, whether Azt/nimbolide can repress tumor growth *in vivo*, we took three different approaches. All *in vivo* approaches were in compliance with institutional and IACUC guidelines. In the first approach, we created flank xenografts using U87EGFRvIII cells and injected Azt or EtoH (control) directly into the tumor bed. In the second approach, we injected nimbolide or DMSO (control) through the tail vein (i.v.) after creating flank xenografts of U87EGFRvIII cells. In the third approach, U87EGFRvIII were seeded orthotopically in the cortex of *Nu/Nu* mice and nimbolide or DMSO (control) was injected (i.v.). In the first model, tumors were allowed to grow for seven days following which 62.5 μl of 95% EtOH or Azt (0.34 μg/g body weight) was injected into the tumor bed of the left and right flank respectively, every other day for eight days. Other than the tumor burden, mice injected with EtOH or Azt were healthy, and did not show lethargy, locomotion or behavioral abnormalities. EtOH exposure caused skin reddening (the reddish area next to the tumor in Fig 6A). Azt, which is extracted with ethanol from leaves is dark green in color and when injected into tumors, gave a dark green hue to tumors (Fig 6A), but did not cause tumor necrosis as judged by histological analysis of tumor sections (Fig 6E, G). However, Azt significantly ($p = 0.00013$) reduced growth of GBM tumors (Fig 6 A-C). Following three injections, the volume of Azt-injected tumors were 50% less than control tumors, while at the end of the study, Azt-treated tumors were less than 10% of the volume of control tumors (Fig 6C).

Histological examination using H&E staining revealed that Azt-treated tumors had markedly reduced cellularity (compare density of nuclei in Fig 6 D & E). Furthermore, Azt markedly reduced the number of tumor cells in different stages of cell division (Fig 6 D, E; arrow heads), while it increased tumor cells with condensed/fragmented chromatin and pycnotic nuclei (indicative of dead cells) (Fig 6 F, G and inset; arrow heads and circle). Immunohistochemistry using Ki67 antibody showed significant ($p = 0.00002$) reduction of proliferative index of Azt-treated tumors (Fig 6 H-J). Azt also caused apoptosis as shown by increased immunoreactivity with cleaved Caspase 3 antibody (Fig 6 K-M). Control tumors overexpressed activated Akt, Erk1/2 and STAT3 as indicated by their phosphorylation status (Fig 6 N, P, R). Importantly, similar to our *in vitro* findings, Azt markedly reduced activation of all three pathways *in vivo* (Fig 6 O, Q, S).

We next examined if systemic administration of nimbolide will be sufficiently bioavailable to have an effect on the growth of flank GBM xenografts. Indeed, compared to DMSO treatment (control), nimbolide (10μg/Kg body wt) had a significant ($p < 0.0001$) inhibitory effect on growth of GBM tumors (Fig 7 A, B). When the study ended (day 11) we observed a three to four fold reduction of tumor volume in nimbolide-treated animals. Many preclinical drugs in trial fail because of their inability to cross the blood brain barrier at quantities sufficient to have an effect on intracranial tumors. Therefore, we examined

whether nimbolide had any effect on orthotopic GBM xenografts. We used three groups of animals – in the first group, we injected U87EGFRvIII cells labeled with lentiviral luciferase, treated mice with DMSO or nimbolide (i.v) every other day (n = 4/subgroup) and measured tumor growth on day 14 (Fig 7C). In the second group, we injected U87EGFRvIII cells labeled DsRed, treated mice with DMSO or nimbolide (i.v) every other day (n = 3/subgroup), euthanized mice on day 14 and monitored tumor growth by measuring tumor area in 2 mm thick coronal brain sections (Fig 7D, E). In the third group, we injected unlabeled U87EGFRvIII cells, treated mice with DMSO or nimbolide (IV) every other day (n = 5/subgroup) and followed survival (Fig 7F). All animals ultimately died; however as revealed by bioluminescence assay (Fig 7C) and fluorescence microscopy of brain sections (Fig 7D), nimbolide reduced tumor growth and prolonged survival of mice (Fig 7E; Log Rank p value 0.017). By measuring tumor area (total area within yellow contour line in D), we found that nimbolide-treated tumors were about 40% smaller relative to DMSO-treated tumors (p value 0.018). Extensive proliferation in GBMs causes metabolic stress leading to necrosis. Nimbolide-injected tumors were not only smaller but also did not show necrosis at the same time point when control tumors showed widespread necrosis (asterisks in Fig 7D). Future studies will be required to determine if nimbolide could be used at higher doses to increase brain bioavailability and if structural modifications of nimbolide could make it more stable, bioavailable and permissive through the brain tissue. The collective results from our three different *in vivo* approaches raise the possibility that either application of nimbolide to the tumor bed post-surgery through wafers and/or systemic administration of a safe, optimized dose of nimbolide could be therapeutically effective in GBM.

DISCUSSION

Glioblastoma multiforme (GBB) remains one of the most lethal forms of human cancers. Less than 5% of patients diagnosed with GBM survive for more than 5 years (26). Despite comprehensive sequencing analysis and our understanding of the core genetic pathways altered in GBM (27), we do not have a clear grasp on the biology of the disease. Targeted therapy has failed so far and conventional standard of care therapy only prolongs progression free survival by about 20% (28). Therefore, there is an urgent need to develop novel therapeutics to treat GBM patients. In this study, our primary objective was to examine the cytotoxic efficacy of Azt and its principal cytotoxic component nimbolide on GBM survival and growth. We demonstrate that Azt/nimbolide, at least *in vitro*, is an extremely potent cytotoxic agent. In fact, after comparing the cytotoxic effects of many other anticancer agents including TMZ, PI3K and mTOR inhibitors, we found that Azt/nimbolide is the most potent of all the agents we have tested so far.

While all GBM cells were susceptible to the cytotoxicity of Azt/nimbolide, those expressing the EGFRvIII oncogene were particularly vulnerability to this agent. The IC50 of nimbolide on this cell was found to be 3.0 μM. Azt/nimbolide halted GBM cells mostly in G1-S. The magnitude of arrest in different cell lines was variable perhaps due to the effect of mutations present in individual glioma cell lines that impact on cell cycle length and progression. The cell cycle effect was robust in the U87EGFRvIII cells as was the extent of RB hypophosphorylation (Fig 4B; 5B) which might partly explain the dramatic G1-S arrest of these cells. Compared to other cells, the U87EGFRvIII cells were also susceptible to lower doses of Azt and nimbolide. Hyperactivation of signaling pathways by oncogenes causes oncogenic stress (29) and cancer cells have evolved mechanisms to counter such stress to remain viable. It is possible that Azt/nimbolide perturbs one or more of these anti-stress pathways in the U87EGFRvIII cells.

Given the fact that Azt/nimbolide had similar cytotoxicity on GBM cells we tested, especially at higher doses, but differential effects on cell cycle and to some extent on RB

phosphorylation, it appears that other mechanisms including a direct impact on survival (as shown by Bcl2 downregulation and PARP cleavage) could also be involved.

Anchorage-independent growth is a classical assay to interrogate invasiveness and metastatic potential of cancer cells (30). U87 and U87EGFRvIII cells are highly invasive *in vivo* (data from many other labs and our own data not shown) and forms colonies *in vitro*. The ability of Azt/nimbolide to prevent colony formation was remarkable and dose-dependent. At the highest dose (20μM nimbolide or 4μg/μl Azt), large colonies were virtually undetectable. This suggests that this agent if retains sufficient systemic activity, might inhibit tissue invasion and metastasis.

The mechanisms of cell death induced by Azt/nimbolide remain unclear. Although the *A. indica* ethanolic extract contains other bioactive components, it is well established that nimbolide is by far the most cytotoxic component (14, 31). Therefore, although it is possible that some of the effects of the extract (Azt) could be potentiated by components other than nimbolide, HPLC analysis and fractionation showed that the most cytotoxic fraction of the extract contained about 2.3% nimbolide (31). Furthermore, we did not observe any additive antiproliferative effect of the extract compared to pure nimbolide. Importantly, the extent of RB hypophosphorylation and rescue of glioma cell proliferation by expression of phosphomimetic RB was very similar in Azt and nimbolide treated cells. Azt/nimbolide caused high to modest apoptosis of cancer cells including HeLa (cervical carcinoma), THP1, U937, HL60, B16 (leukemia) (32, 21) and HT29 (colon cancer) cells (22). In one study Azt/nimbolide caused apoptosis in leukemia, lymphoma, human embryonic kidney, multiple myeloma, breast cancer and human squamous cell carcinoma by suppressing cytokine-induced NF-κB activation (20). In our study, Azt/nimbolide caused extensive apoptosis *in vitro* as well as *in vivo*. Downstream of PI3K, Akt plays a major role in promoting cell survival by stabilizing the Bcl2 protein (33) and increasing its transcription (34). It is possible that akin to other studies (17) downregulation of Bcl2 by Azt/nimbolide in GBM cells is due to its inhibitory action of Akt phosphorylation.

Signaling pathways frequently deregulated in GBM include the EGFR/EGFRvIII-driven PI3K-Akt pathway, RAS-MAP kinase pathway, JAK-STAT pathway and the RB pathway (4, 27). It is therefore remarkable that Azt/nimbolide suppressed all these pathways with the greatest effect observed in GBM cells expressing the EGFRvIII oncogene. Azt/nimbolide did show some specificity since it suppressed the above pathways without inhibiting mTOR and without changing the total protein levels of several cell cycle regulators including Cyclin D, Cyclin B, P27 and P21. The three adult GBM cells that we primarily used in this study are all homozygous null for the G1-S cell cycle inhibitor INK4a/ARF (CDKN2A in humans) that inhibits CDK4/6, the primary kinase that phosphorylates and inactivates RB. Absence of INK4a/ARF therefore leads to unchecked CDK4/6 activity in these GBM cells. Thus, it is of high significance that Azt/nimbolide directly inhibits CDK4/6 activity leading to RB hypophosphorylation and G1-S arrest, particularly in GBM cells expressing the oncogene EGFRvIII.

Studies showing the *in vivo* cytotoxicity of Azt/nimbolide are limited. The LD_{50} of Azt was found to be 4.57 mg/g body weight in acute toxicity studies in rodents (35). In this study we found that acute exposure of GBM cells *in vitro* to Azt prevents tumor formation *in vivo*. We attempted to bring Azt to a water-soluble form, but the resulting extract following EtOH evaporation was ineffective in killing GBM cells *in vitro*. Therefore, we had to rely on the EtOH-soluble fraction for *in vivo* studies. We however, demonstrated that intratumor injection of a very low dose of Azt (0.34 μg/g body weight) considerably suppressed tumor growth. Importantly, we also show that systemic administration of nimbolide, the principal cytotoxic component of Azt can significantly inhibit GBM grown both in flank and

intracranial orthotopic glioma models. Grade IV gliomas or GBMs are histologically characterized by hypercellularity and presence of extensive mitotic activity. Azt reduced hypercellularity, inhibited proliferation and induced apoptosis in GBM tumor xenografts. It also inhibited growth factor signaling *in vivo* as revealed by the reduced staining of phosphorylated Akt, Erk1/2 and STAT3 in Azt injected tumors.

In summary, our results demonstrate that Azt/nimbolide is a potent cytotoxic agent that exerts antiproliferative and apoptotic effect in GBM *in vitro* and *in vivo*. It suppresses GBM viability and suppresses tumor growth by inhibiting CDK4/6 activity leading to RB hypophosphorylation and cell cycle arrest and by inhibiting growth factor pathways hyperactivated in GBM including the PI3K-Akt, MAP kinase and JAK-STAT pathways. Further studies are needed to explore solubility of Azt in aqueous solutions, examine the bioavailability of Azt and nimbolide and determine their therapeutic efficacy as a single agent or in combination with chemotherapy and radiation in orthotopic mouse models of human GBM and other cancers.

Supplementary Material

Refer to Web version on PubMed Central for supplementary material.

Acknowledgments

We thank Paul Mischel, UCLA for U87EGFR and U87EGFRvIII cells, Peter Houghton, Nationwide Children's Hospital, Columbus, OH for the G2 cells and John Ohlfest, University of Minnesota for the P9 neurosphere line. This work was supported by NIH/NHLBI R01HL111192 (to AK), and the Division of Oncology, CCHMC, CancerFreeKids, CCHMC Trustee Scholar grant and NIH/NINDS R01NS075291 (to BD).

Financial Support: This work was supported by the Division of Oncology, CCHMC, CancerFreeKids, CCHMC Trustee Scholar grant and NIH R01NS075291.

REFERENCES

1. Wong AJ, Ruppert JM, Bigner SH, Grzeschik CH, Humphrey PA, Bigner DS, et al. Structural alterations of the epidermal growth factor receptor gene in human gliomas. Proc Natl Acad Sci USA. 1992; 89:2965–9. [PubMed: 1557402]
2. Rasheed BK, McLendon RE, Friedman HS, Friedman AH, Fuchs HE, Bigner DD, et al. Chromosome 10 deletion mapping in human gliomas: a common deletion region in 10q25. Oncogene. 1995; 10:2243–6. [PubMed: 7784070]
3. Ueki K, Ono Y, Henson JW, Efird JT, von Deimling A, Louis DN. CDKN2/p16 or RB alterations occur in the majority of glioblastomas and are inversely correlated. Cancer Res. 1996; 56:150–3. [PubMed: 8548755]
4. Heldin CH. Protein tyrosine kinase receptors. Cancer Surv. 1996; 27:7–24. [PubMed: 8909792]
5. Manson MM. Inhibition of survival signalling by dietary polyphenols and indole-3-carbinol. Eur J Cancer. 2005; 41:1842–53. [PubMed: 16087329]
6. Visanji JM, Duthie SJ, Pirie L, Thompson DG, Padfield PJ. Dietary isothiocyanates inhibit Caco-2 cell proliferation and induce G2/M phase cell cycle arrest, DNA damage, and G2/M checkpoint activation. J Nutr. 2004; 134:3121–6. [PubMed: 15514285]
7. Khan N, Afaq F, Mukhtar H. Cancer chemoprevention through dietary antioxidants: progress and promise. Antioxidants & redox signal. 2008; 10:475–510.
8. Karmakar S, Banik NL, Patel SJ, Ray SK. Garlic compounds induced calpain and intrinsic caspase cascade for apoptosis in human malignant neuroblastoma SH-SY5Y cells. Apoptosis. 2007; 12:671–84. [PubMed: 17219050]
9. Germano G, Frapolli R, Belgiovine C, Anselmo A, Pesce S, Liguori M, et al. Role of macrophage targeting in the antitumor activity of trabectedin. Cancer Cell. 2013; 23:249–62. [PubMed: 23410977]

10. Keating, B. Neem: The Miraculous Healing Herb. The Neem Association; Winter Park, FL: 1994.
11. Subapriya R, Nagini S. Medicinal properties of neem leaves: a review. Curr Med Chem Anti-cancer agents. 2005; 5:149–6.
12. Anyaehie UB. Medicinal properties of fractionated acetone/water neem [Azadirachta indica] leaf extract from Nigeria: a review. Nigerian journal of physiological sciences: official publication of the Physio Soc Nigeria. 2009; 24:157–9.
13. Udeinya IJ, Mbah AU, Chijioke CP, Shu EN. An antimalarial extract from neem leaves is antiretroviral. Trans Royal Soc Tropical Med and Hyg. 2004; 98:435–7.
14. Sastry BS, Suresh Babu, K Hari, Babu T, Chandrasekhar S, Srinivas PV, Saxena AK, et al. Synthesis and biological activity of amide derivatives of nimbolide. Bioorg & Medicin Chem Lett. 2006; 16:4391–4.
15. Suresh G, Gopalakrishnan G, Wesley SD, Pradeep Singh ND, Malathi R, Rajan SS. Insect antifeedant activity of tetranortriterpenoids from the Rutales. A perusal of structural relations. J Agri Food Chem. 2002; 50:4484–90.
16. Rochanakij S, Thebtaranonth Y, Yenjai C, Yuthavong Y. Nimbolide, a constituent of Azadirachta indica, inhibits Plasmodium falciparum in culture. Southeast Asian J of Trop Med and Public Health. 1985; 16:66–72. [PubMed: 3895455]
17. Harish Kumar G, Vidya Priyadarsini R, Vinothini G, Vidjaya Letchoumy P, Nagini S. The neem limonoids azadirachtin and nimbolide inhibit cell proliferation and induce apoptosis in an animal model of oral oncogenesis. Invest New Drugs. 2010; 28:392–401. [PubMed: 19458912]
18. Cohen E, Quistad GB, Casida JE. Cytotoxicity of nimbolide, epoxyazadiradione and other limonoids from neem insecticide. Life Sci. 1996; 58:1075–81. [PubMed: 8622560]
19. Harish Kumar G, Chandra Mohan KV, Jagannadha Rao A, Nagini S. Nimbolide a limonoid from Azadirachta indica inhibits proliferation and induces apoptosis of human choriocarcinoma (BeWo) cells. Invest New Drugs. 2009; 27:246–52. [PubMed: 18719855]
20. Gupta SC, Prasad S, Reuter S, Kannappan R, Yadav VR, Ravindran J, et al. Modification of cysteine 179 of IkappaBalpha kinase by nimbolide leads to down-regulation of NF-kappaB-regulated cell survival and proliferative proteins and sensitization of tumor cells to chemotherapeutic agents. J Biol Chem. 2010; 285:35406–17. [PubMed: 20829362]
21. Roy MK, Kobori M, Takenaka M, Nakahara K, Shinmoto H, Isobe S, et al. Antiproliferative effect on human cancer cell lines after treatment with nimbolide extracted from an edible part of the neem tree (Azadirachta indica). Phytotherapy Res: PTR. 2007; 21:245–50.
22. Roy MK, Kobori M, Takenaka M, Nakahara K, Shinmoto H, Tsushida T. Inhibition of colon cancer (HT-29) cell proliferation by a triterpenoid isolated from Azadirachta indica is accompanied by cell cycle arrest and up-regulation of p21. Planta Med. 2006; 72:917–23. [PubMed: 16858664]
23. Subapriya R, Kumaraguruparan R, Nagini S. Expression of PCNA, cytokeratin, Bcl-2 and p53 during chemopreventionof hamster buccal pouch carcinogenesis by ethanolic neem (Azadirachta indica) leaf extract. Clin. Biochem. 2006; 39:1080–87. [PubMed: 16989797]
24. Dasgupta B, Milbrandt J. AMP-activated protein kinase phosphorylates retinoblastoma protein to control mammalian brain development. Dev Cell. 2009; 16:256–70. [PubMed: 19217427]
25. Véronique Mathieu V, De Nève N, Le Mercier M, Dewelle J, Gaussin J, Dehoux M, Kiss R, Lefranc F. Combining Bevacizumab with Temozolomide Increases the Antitumor Efficacy of Temozolomide in a Human Glioblastoma Orthotopic Xenograft Model. Neoplasia. 2008; 10:1383–92. [PubMed: 19048117]
26. Dolecek TA, Propp JM, Stroup NE, Kruchko C. CBTRUS statistical report: primary brain and central nervous system tumors diagnosed in the United States in 2005-2009. Neuro-oncol. 2012; 14(Suppl 5):v1–49. [PubMed: 23095881]
27. Maher EA, Furnari FB, Bachoo RM, Rowitch DH, Louis DN, Cavenee WK, et al. Malignant glioma: genetics and biology of a grave matter. Genes & Dev. 2001; 15:1311–33. [PubMed: 11390353]
28. Balmaceda C, Peereboom D, Pannullo S, Cheung YK, Fisher PG, Alavi J, et al. Multi-institutional phase II study of temozolomide administered twice daily in the treatment of recurrent high-grade gliomas. Cancer. 2008; 112:1139–46. [PubMed: 18246536]

29. Dengler MA, Staiger AM, Gutekunst M, Hofmann U, Doszczak M, Scheurich P, et al. Oncogenic stress induced by acute hyper-activation of Bcr-Abl leads to cell death upon induction of excessive aerobic glycolysis. PloS one. 2011; 6:e25139. [PubMed: 21949869]

30. Nikiforov MA, Hagen K, Ossovskaya VS, Connor TM, Lowe SW, Deichman GI, et al. p53 modulation of anchorage independent growth and experimental metastasis. Oncogene. 1996; 13:1709–19. [PubMed: 8895517]

31. Cohen E, Quistad GB, Jefferies PR, Casida JE. Nimbolide is the principal cytotoxic component of neem-seed insecticide preparations. Pestic. Sci. 1996; 48:135–140.

32. Priyadarsini RV, Murugan RS, Sripriya P, Karunagaran D, Nagini S. The neem limonoids azadirachtin and nimbolide induce cell cycle arrest and mitochondria-mediated apoptosis in human cervical cancer (HeLa) cells. Free Rad Res. 2010; 44:624–34.

33. Datta SR, Dudek H, Tao X, Masters S, Fu H, Gotoh Y, et al. Akt phosphorylation of BAD couples survival signals to the cell-intrinsic death machinery. Cell. 1997; 91:231–41. [PubMed: 9346240]

34. Pugazhenthi S, Nesterova A, Sable C, Heidenreich KA, Boxer LM, Heasley LE, et al. Akt/protein kinase B up-regulates Bcl-2 expression through cAMP-response element-binding protein. J Biol Chem. 2000; 275:10761–6. [PubMed: 10753867]

35. Chattopadhyay RR. Possible biochemical mode of anti-inflammatory action of Azadirachta indica A. Juss. in rats. Ind Exp Biol. 1998; 36:418–20.

TRANSLATIONAL RELEVANCE

Despite our understanding of the core genetic pathways of GBM and despite considerable advancement in therapy and success in other cancers, the median survival in GBM ranges from 9 to 12 months. Decades of surgical therapy, chemotherapy and radiotherapy have essentially failed to significantly change the outcome of the disease. Therefore, there is a desperate need to find new approaches that might work together with standard of care therapy to improve survival of GBM patients. In our study, we demonstrate that Azt/nimbolide is a very potent agent in glioblastoma. In fact, we found that at least *in vitro*, this agent is more cytotoxic than nearly all small molecules currently being tested in GBM preclinical models. It also inhibited tumor progression *in vivo*. GBM is characterized by hyperactivation of multiple growth factor pathways and Azt/nimbolide inhibited three key growth factor pathways relevant in GBM. A vitally important issue will be to conduct more rigorous and extensive analysis to determine the bioavailability, pharmacokinetics and pharmacodynamics of nimbolide and improve blood-brain-barrier diffusion of this potent cytotoxic agent.

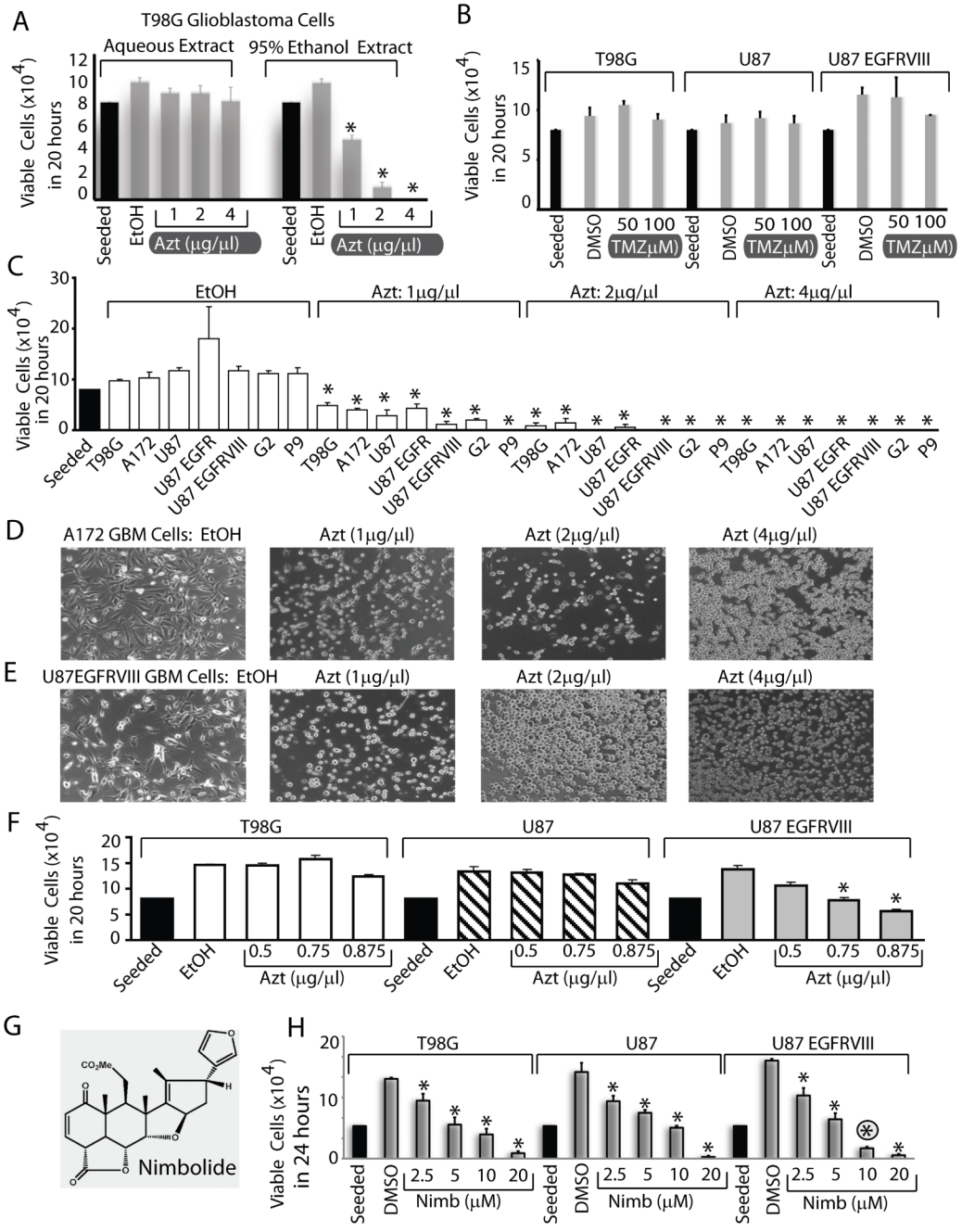

Figure 1. Azt/ nimbolide is a potent cytotoxic agent in Glioblastoma

(A) Cytotoxic effect of aqueous or EtOH extracts (Azt) of *Azadirachta indica* on T98G human glioblastoma (GBM) cells (A) and that of Temozolomide (TMZ) on T98G, U87 and U87EGFRvIII cells (B). (C) Dose-dependent cytotoxicity of Azt in a panel of human GBM cells treated with Azt or ethanol (control) for 20 hours. (D, E) Photomicrographs showing morphology of GBM cells (control-EtOH treated, attached) but lifting from tissue culture plates following Azt treatment for 20h. (F) GBM cells expressing the EGFRvIII oncogene are sensitive to lower doses of Azt than parental cells. Cytotoxicity of nimbolide (G), the principal cytotoxic component of Azt on a panel of GBM cells (H). Note: U87 EGFRvIII

cells are more sensitive to 10μM nimbolide (circled asterisk). Data is representative of two to four experiments. *$p \leq 0.001$.

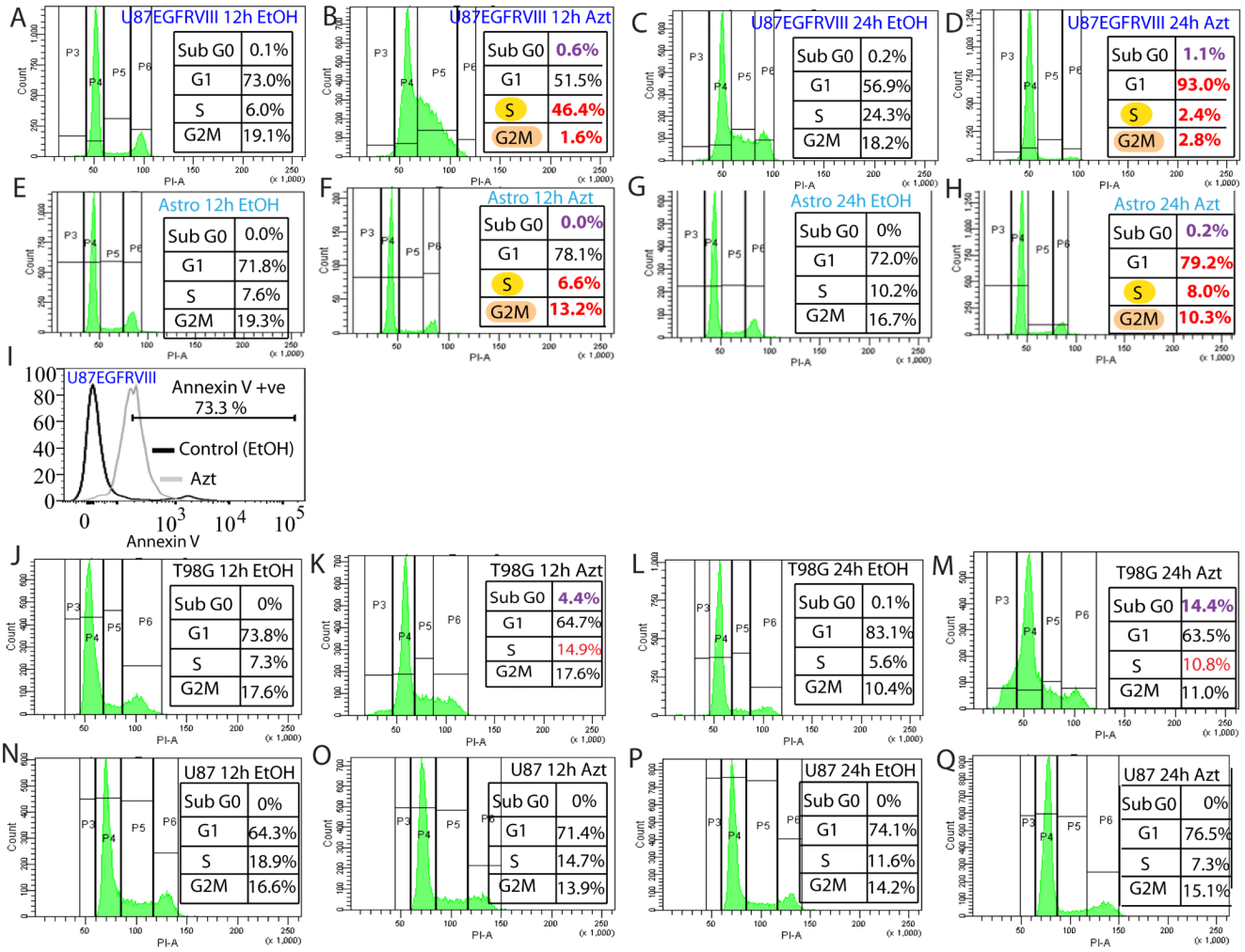

Figure 2. Azt/nimbolide arrests GBM cells at G1-S

Flow cytometry using PI showing the effect of Azt/nimbolide on cell cycle of U87EGFRvIII cells (A-D), astrocytes (E-H), and Annexin V staining showing apoptosis of Azt-treated U87EGFRvIII cells (I) is shown. Effects of Azt on cell cycle of T98G cells (J-M) and U87 cells (N-Q) are also shown. Note that Azt treatment caused complete depletion of U87EGFRvIII cells from G2M at 12 hours and nearly 100% G1 arrest at 24 hours. Data is representative of three independent experiments. U87

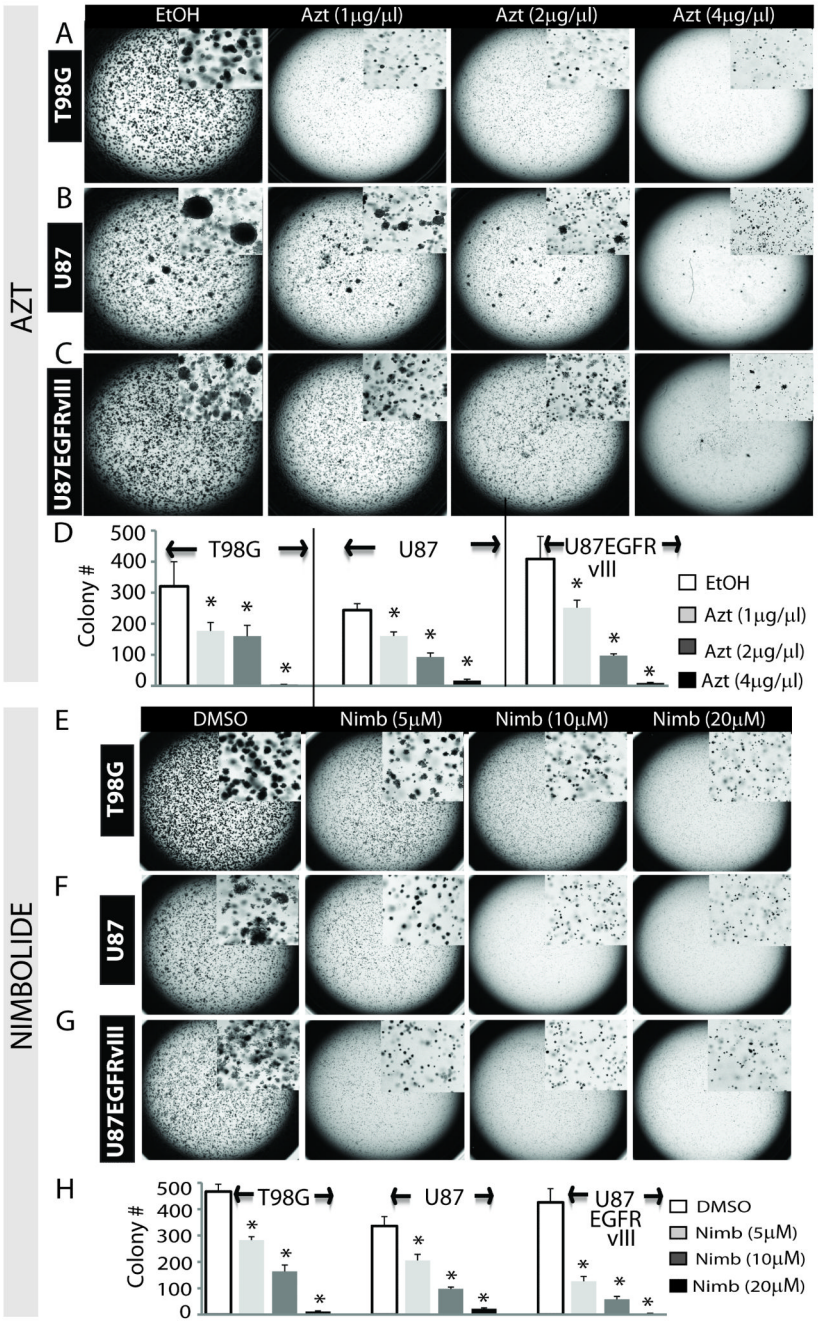

Figure 3. Azt/nimbolide inhibits anchorage-independent growth of GBM cells

Photomicrographs showing colony formation of T98G cells (A), U87 cells (B) and U87EGFRvIII cells (C) grown in the presence of EtOH (control) or Azt for two weeks. Inset shows magnified view of the colonies. (D) Quantitation of colony counts in A-C. Similar experiments were done using various doses of nimbolide or DMSO (control). Colony formation of the same cells are shown in E-G. Quantitation of colony counts in E-G is shown in H. Inset shows magnified view of the colonies. *$p \leq 0.001$.

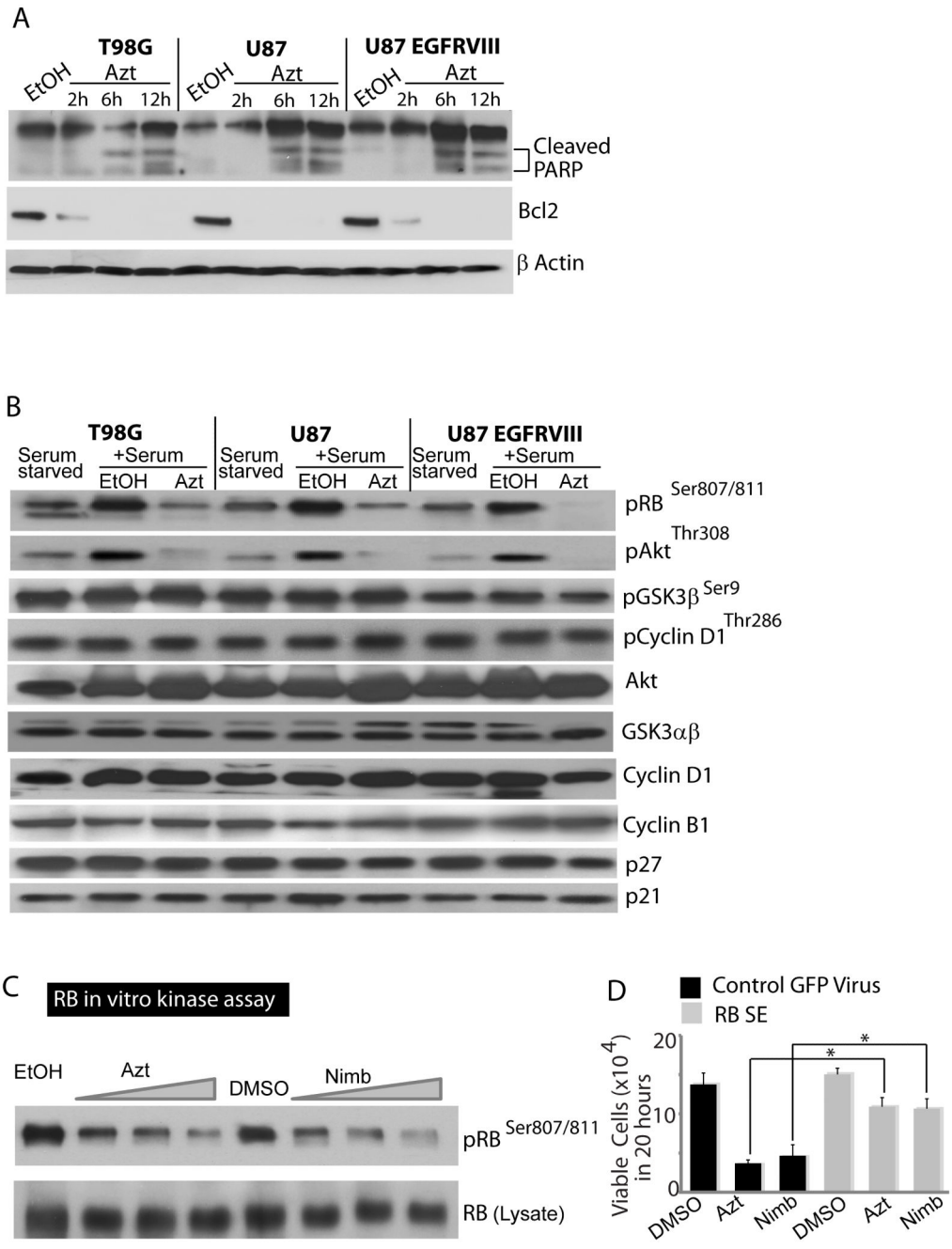

Figure 4. Azt/nimbolide induces apoptosis, downregulates Bcl2, inhibits Akt and CDK4/6 kinase activity

(A) Immunoblots showing the dose-dependent effects of Azt in induction of apoptosis (note: smaller bands of PARP cleaved by active Caspases at 6 & 12h of Azt treatment), and down regulation of Bcl2. Actin was used as a loading control. (B) Immunoblots showing RB and Akt phosphorylation by serum in serum-starved GBM cells and inhibition of phosphorylation by Azt but not by EtOH (control). Phosphorylation state of Akt substrate GSK3β, GSK3β substrate Cyclin D1 and total levels of GSK3αβ, Akt, Cyclin D1, Cyclin B1, p21 and p27 are also shown (note; Azt did not change total levels of proteins or that of G1-S cell cycle inhibitors p21 and p27). (C) *In vitro* kinase assay showing dose-dependent

inhibition of CDK4/6 activity by Azt (1, 2 and 4μg/μl) and nimbolide (5, 10 and 20μM) but not by EtOH or DMSO (vehicle controls). (D) Rescue experiment showing the effect of Azt and nimbolide on the proliferation of U87EGFRvIII cells transduced with control lentivirus or lentivirus expressing phosphomimetic RB. Data is representative of two to four independent experiments.

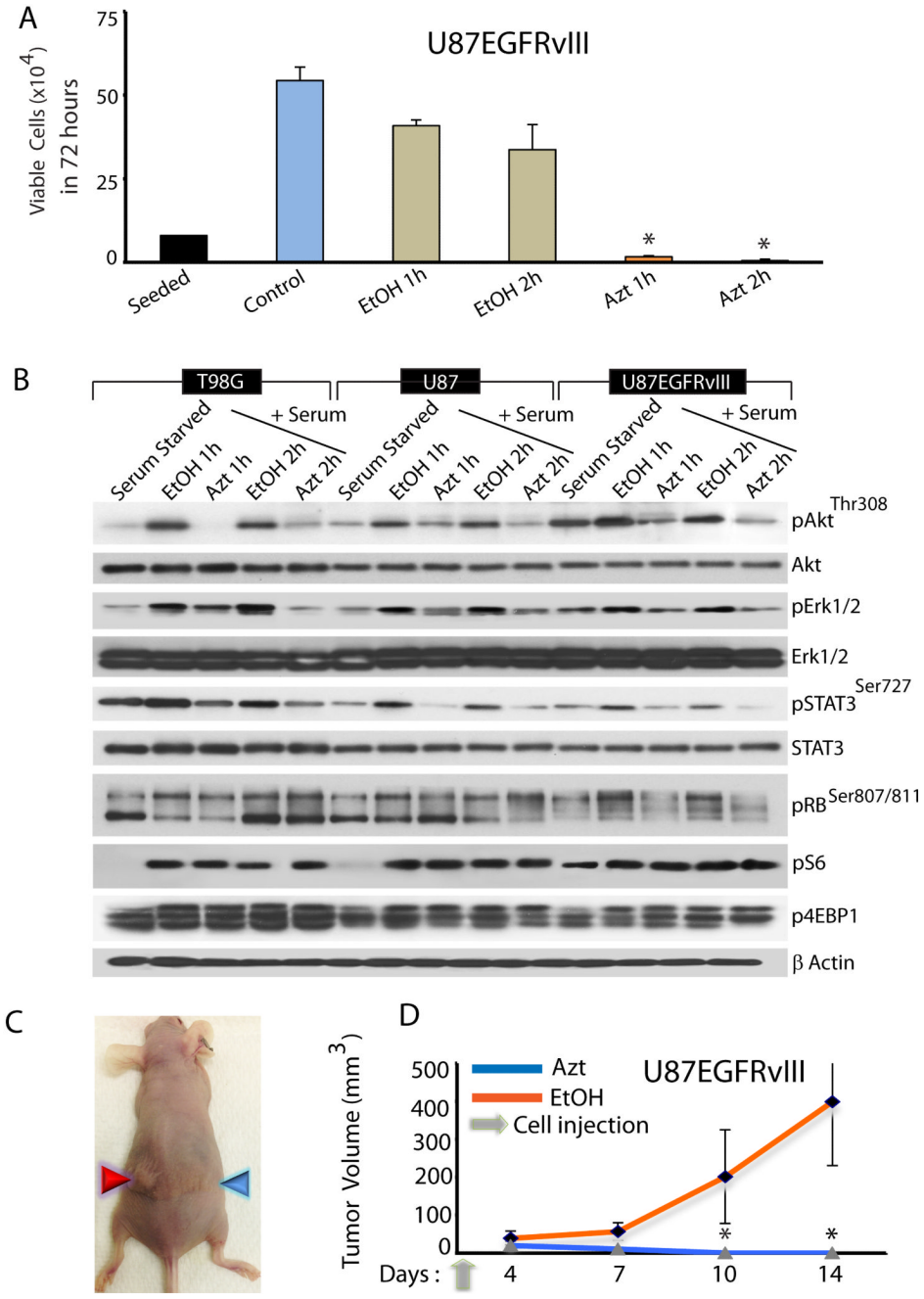

Figure 5. Cytotoxicity of Azt/nimbolide is irreversible

(A) Growth assay showing viability of U87EGFRvIII cells following pre-treatment with medium (control), EtOH (control) or Azt (2μg/μl). (B) Immunoblot analysis showing activation of growth factor pathways by serum and acute inhibition of the pathways by Azt/nimbolide. Note: phosphorylation of Akt, Erk1/2 and STAT3 and RB by serum in the presence of EtOH (control) and robust inhibition of phosphorylation in the presence of Azt. Also note that mTORC1 activation, indicated by phosphorylation of S6 and 4EBP1 is unaffected by Azt. Actin was used as a loading control. Data is representative of at least three independent experiments. (C) Representative digital photograph showing tumor growth in mice injected with EtOH-pretreated (red arrowhead) or Azt-pretreated (blue

arrowhead) U87EGFRvIII cells. (D) Growth of tumor xenografts in *Nu/Nu* mice (n=8) initiated by U87EGFRvIII cells pretreated with EtOH or Azt. Tumor volume was measured at indicated time points and the mean tumor volume was calculated. *$p \leq 0.0002$.

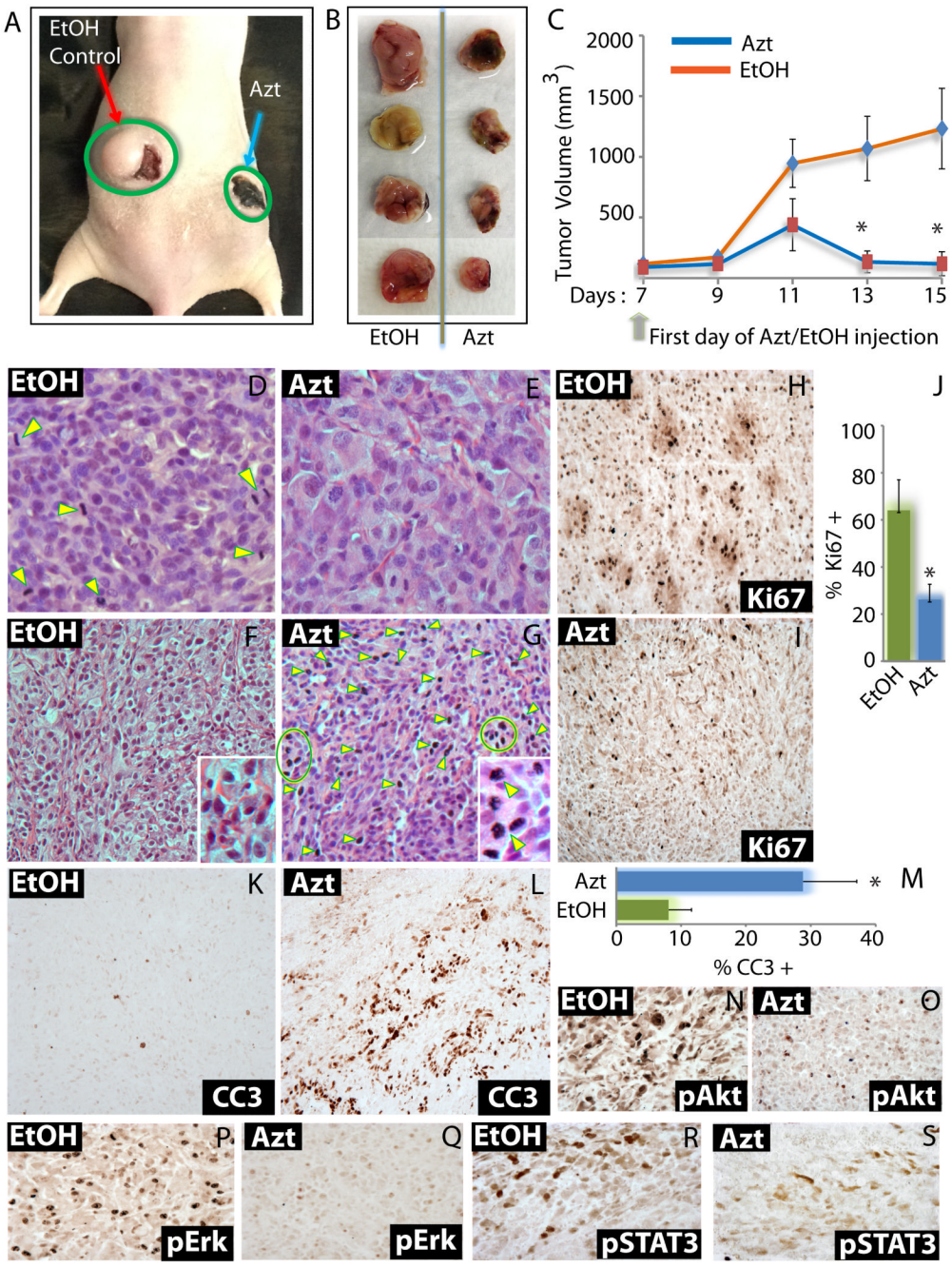

Figure 6. Administration of Azt/nimbolide into tumor bed suppresses tumor growth

(A) Representative digital photograph showing U87EGFRvIII tumor growth in mice injected with EtOH (red arrow) or Azt (blue arrow). (B) Digital photographs of tumors injected with EtOH or Azt were dissected out at the end of the experiment. (C) Growth of tumor xenografts in *Nu/Nu* mice (n=8) initiated by U87EGFRvIII cells and treated with EtOH or Azt. Treatment started following tumor growth for seven days. Injection schedule and tumor volume measurement at indicated days are shown. (D-G) H&E of tumors injected with EtOH or Azt. Note: Cells in different stages of cell division (yellow arrowheads) in (D) which is significantly reduced in (E), and marked increase in cells with condensed/ fragmented chromatin and pycnotic nuclei (indicative of dead cells) in (G) compared to (F).

Immunohistochemistry using Ki67 antibody showing proliferating cells (H, I), quantitation of Ki67+ cells (J), using cleaved Caspase 3 (CC3) antibody showing apoptotic cells (K, L) and quantitation of CC3+ cells (M) in EtOH and Azt treated tumors. Immunohistochemistry showing phosphorylated levels of Akt (N, O), Erk1/2 (P, Q) and STAT3 (R, S) in EtOH and Azt treated tumors. *$p < 0.0001$.

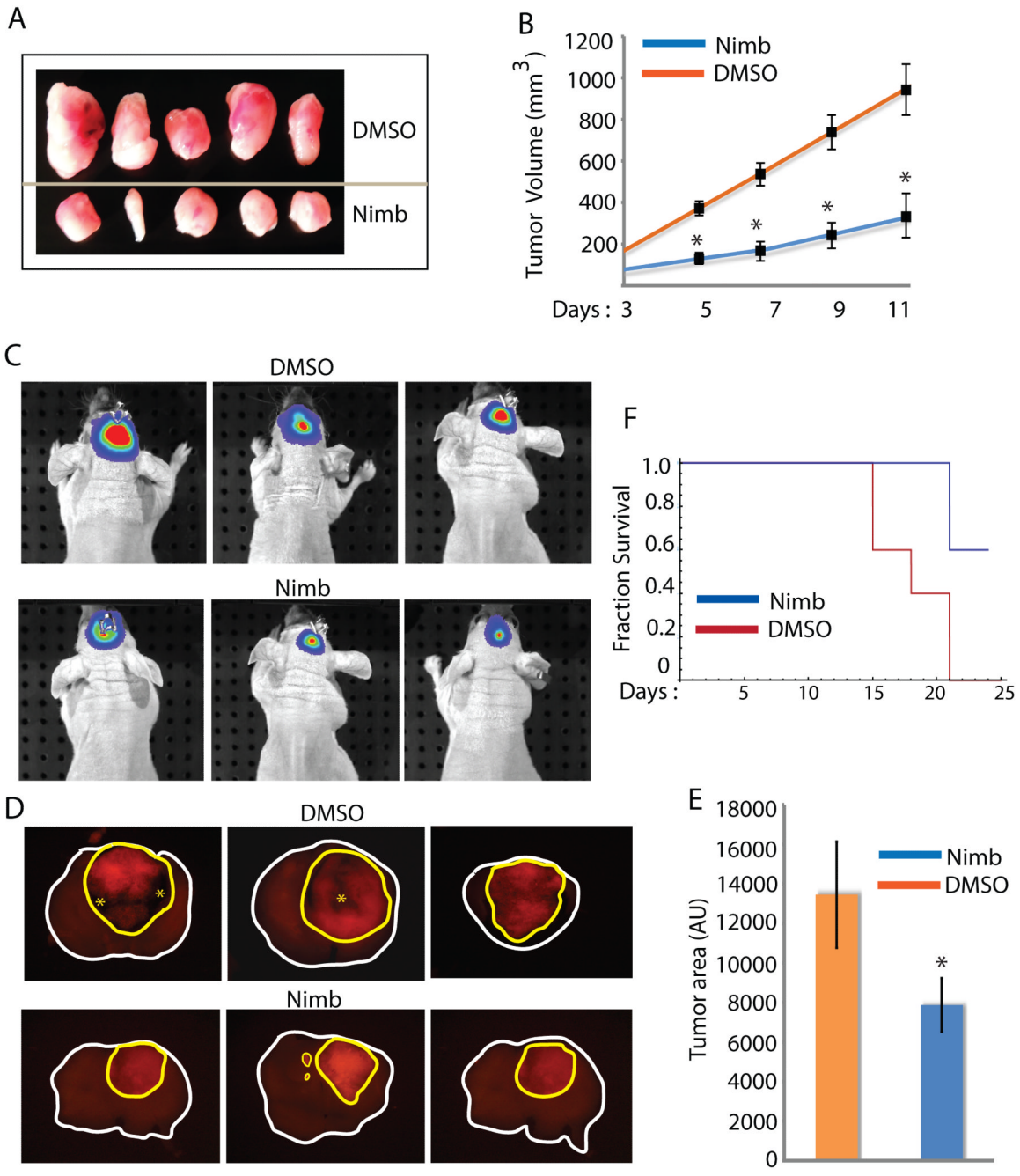

Figure 7. Azt/nimbolide suppresses tumor growth *in vivo*

(A) Digital photographs of tumors from mice treated with DMSO or nimbolide. (B) Growth analysis of tumor xenografts in *Nu/Nu* mice initiated by U87EGFRvIII cells and treated with EtOH or Azt (*$p < 0.0001$). (C) Bioluminescence signal of intracranial tumors of three representative mice treated with DMSO or nimbolide and measured on day 14. (D) DsRed Fluorescence signal from coronal sections of intracranial gliomas prepared from mice treated with DMSO or nimbolide. Tumors are circled in yellow; asterisks represent necrosis. (E) Quantification of tumor area from (D). (F) Kaplan-Meier survival analysis of intracranial tumor-bearing mice treated with DMSO or nimbolide (Log Rank p value 0.017).